Icephobic performance on the aluminum foil-based micro-/nanostructured surface*

Yu Chen(陈宇)[1,†], Guicheng Liu(刘桂成)[2,†,‡], Lei Jiang(姜磊)[3], Ji Young Kim(金志永)[2], Feng Ye(叶锋)[4], Joong Kee Lee(李重基)[2], Lei Wang(王磊)[5,§], and Bo Wang(王波)[1,¶]

[1] *College of Materials Science and Engineering, Beijing University of Technology, Beijing* 100124, *China*
[2] *Center for Energy Convergence Research, Green City Research Institute, Korea Institute of Science and Technology (KIST), Hwarang-ro* 14-*gil* 5, *Seongbuk-gu, Seoul* 02792, *Republic of Korea*
[3] *Industrial Centre, The Hong Kong Polytechnic University, Hung Hom, Kowloon, Hong Kong, China*
[4] *State Key Laboratory of Multiphase Complex Systems, Institute of Process Engineering, Chinese Academy of Sciences, Beijing* 100190, *China*
[5] *Key Laboratory of Cryogenics, Technical Institute of Physics and Chemistry, Chinese Academy of Sciences, Beijing* 100190, *China*

(Received 5 December 2016; revised manuscript received 10 January 2017; published online 20 February 2017)

The research of superhydrophobic materials has attracted many researchers' attention due to its application value and prospects. In order to expand the serviceable range, people have investigated various superhydrophobic materials. The simple and easy preparation method has become the focus for superhydrophobic materials. In this paper, we present a program for preparing a rough surface on an aluminum foil, which possesses excellent hydrophobic properties after the treatment with low surface energy materials at high vacuum. The resulting contact angle is larger than 160°, and the droplet cannot freeze on the surface above −10 °C. Meanwhile, the modified aluminum foil with the thickness of less than 100 μm can be used as an ideal flexible applied material for superhydrophobicity/anti-icing.

Keywords: aluminum foil, micro-nanostructure, superhdrophobicity, anti-icing, flexibility

PACS: 68.03.Cd, 68.08.–p, 68.35.Ct, 68.35.Np **DOI:** 10.1088/1674-1056/26/4/046801

1. Introduction

Influenced by the lotus leaf, many researchers began to divert their attention to bionic manufacturing and the secondary structure has become the focus of the study.[1–6] Superhydrophobic surfaces, with water contact angle larger than 150°, and the sliding angle lower than 5°, have attracted attention of researchers due to their applications in different fields, such as anti-icing, anti-fogging, and self-cleaning.[7–13] The reasons for superhydrophobicity are caused by two aspects: rough structure on multiple scales and low surface energy coatings. The rough structure could enhance the air-trapping, leading to the discontinuity of the three phases, which impels the droplet to roll off the surface easily. Foreign matters on the surface could be whirled away by the rolling droplet. Correspondingly, the nanolayer coating with various microstructures, as a classic way, has been widely used to enhance the rough degree of the substrate surface.[14–17] The traditional coating material and preparation method are metal oxide, for example, ZnO,[18,19] and hydrothermal reaction technology.[20–22]

In recent years, many research studies have been done on fabricating superhydrophobic surfaces, including hydrothermal methods, vapor deposition, magnetron sputtering, soft-lithography, replica molding, etc.[23–28] Replica molding is one of the most useful and easy methods for fabricating microstructure on a material's surface. So far, this method has been widely used in bio-fabrication for replicating the surfaces in nature,[29–31] such as plant leaves and insects' special structure on the surface. Also the general material used as replicating model is PDMS. But aluminum foil as a soft material has been rarely used for replicating models, which may become a wide range of applications.[32–36]

The research for superhydrophobic materials has attracted many researchers' attention because of its high application value and good prospects. In order to expand their utilization range, researchers began to study other functions based on superhydrophobicity, e.g., directional moving, anti-icing, anti-fogging, etc.[37–40] Meanwhile, the flexible device is also becoming a research hot-point in recent years.[41–43] Preparation for special functional surfaces by a simple and easy method has become the focus. This article describes a program for fabricating rough structures on aluminum foil by machining and crystal growth methods, which holds excellent hydropho-

*Project supported by China Postdoctoral Science Foundation (Grant No. 2016M590137), the National Natural Science Foundation of China (Grant No. 21476246), the Youth Innovation Promotion Association of the Chinese Academy of Sciences (Grant No. 2016047), the KIST Institutional Program (Grant No. 2E26291), and Research Grants of NRF funded by the National Research Foundation under the Ministry of Science, ICT & Future, Korea (Grant No. NRF-2015H1D3A1036078).

† These authors contributed equally to this work.
‡Corresponding author. E-mail: log67@163.com
§Corresponding author. E-mail: silu861004@163.com
¶Corresponding author. E-mail: wangbo@bjut.edu.cn

© 2017 Chinese Physical Society and IOP Publishing Ltd

bic properties after the treatment with trimethoxysilane under high vacuum condition. The contact angle is larger than 160°, and the droplet could not freeze in a short time on the surface at −10 °C. Moreover, a droplet on the surface can be driven off easily after melting, which is mainly caused by enhanced micro-/nano-structured surface. The thickness of modified aluminum foil is less than 100 μm, which will become an ideal flexible material for engineering.

2. Materials and methods

An aluminum foil with thickness of 0.1 mm and other chemical materials were purchased from Beijing Lan Yi products and chemical Co., Ltd., China. The micro structure was prepared by a steel template using a hexamethylene tetramine, $Zn(NO_3)_2$, as a modification solution. A steel template (20.0 mm×10.0 mm×2 mm) was machined to form the micro-scale sawtooth with a periodicity of 400 μm, the sawtooth height of 50 μm. We put the aluminum foil on the template surface after it was folded once, and then the micro structure appeared by pressing hard on the aluminum foil surface with a rubber hummer. The micro structure surface was cleaned with ultrasonic cleaner in deionized water and ethanol for 10 min, respectively, and then we dried the sample in an oven. We dipped the samples into crystal seed liquid and burnt them at 300 °C for 3 min for coating crystal seed. The crystal seed liquid was prepared as follows: 4-g $Zn(Ac)_2{\cdot}2H_2O$, 20-mL ethylene glycol monomethyl ether, and 0.9-g monoethanolamine were mixed and stirred with a magnetic stirrer for 10 min. On the other hand, the nanostructure was produced by a simple chemical reaction, which was exactly a corrosion reaction. The reaction solution was prepared as follows: 0.10-g $Zn(NO_3)_2{\cdot}6H_2O$ and 0.52-g hexamethylene tetramine were mixed into 100-mL deionized water, and stirred until the solution became transparent. The samples were put into a Teflon reactor at 90 °C for 12 h to realize the surface with nano-/micro-structure. The surface was washed after it was removed from the reactor with deionized water and ethanol respectively, and then put it into an oven for drying. The surface was cleaned with plasma cleaning (PDC-32G, HARRICK PLSMA) at appropriate power for 15 min and enhanced the chemical activities. The samples were moved into a vacuum dryer with 3–4 drops of Heptadeca Fluorodecyltri-propoxysilane (FAS-17). We closed the valve after creating the vacuum for 15 min, and then moved the vacuum dryer into an oven at 70 °C for 6 h. The sample obtained an ultra-low-energy surface after it was modified by the Heptadeca Fluorodecyltri-propoxysilane. Therefore, it displayed superhydrophobic/anti-icing properties.

3. Results and discussion

3.1. Characterization of the patterns

Figure 1(a) shows the schematic diagram of the fabrication process described in the experimental section. Figures 1(b)–1(e) indicate the topography of the surface composed of micro-ratchets and nano-petals (MN-surface). The micro-scale sawtooth with a periodicity of 400 μm observed by the scanning electron microscope (SEM) test, as shown in Figs. 1(b) and 1(c), provides much more pocketed air between solid and liquid interface, resulting in inducing the droplet to be in Cassie's state. The magnified view of the surface is shown in Figs. 1(d) and 1(e). The results show that the surface was successfully covered with nano-petals that can effectively enhance the roughness and lower the adhesion force between the liquid and solid interface.

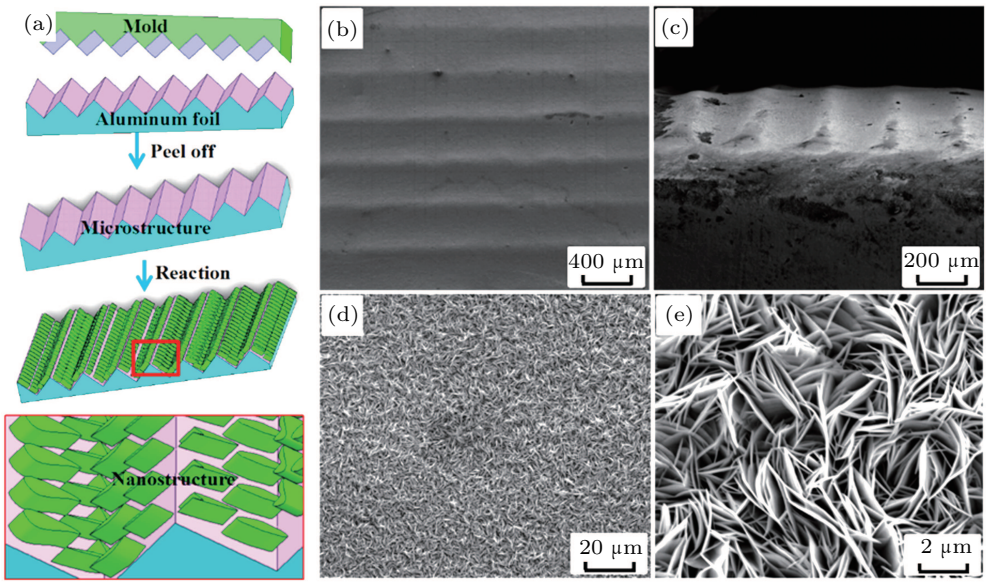


Fig. 1. (color online) The sketch of the fabrication process and scanning electron microscope (SEM) images of the topography. (a) Schematic diagram of the fabrication process. (b) and (c) The top view and side view of the topography with the micro-sawtooth space of 400 μm. (d) and (e) The magnified view of the surface composed with ZnO nano-petals.

3.2. X-ray diffraction and wettability test

To identify the element of the topography, we observe the surface via an x-ray diffraction (XRD). Two surfaces are used to contrast, i.e., an aluminum foil and the MN-surface. To compare the difference between the the aluminum foil (Fig. 2(a)) and the MN-surface (Fig. 2(b)). The XRD analysis is used to determine the phase compositions for the aluminum foil and the MN-surface. The results indicate that the aluminum foil surface was coated by a layer of ZnO nanopetals after the hydrothermal treatment. The main composition on the aluminum foil surface is replaced by the ZnO.

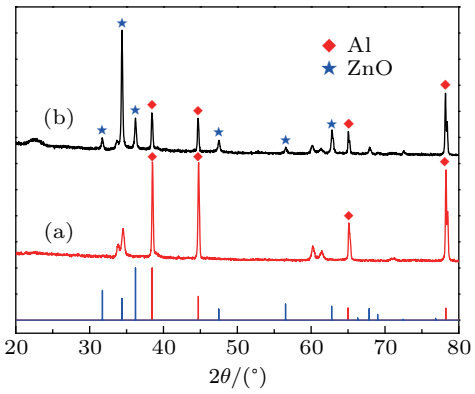


Fig. 2. (color online) The x-ray diffraction (XRD) test of (a) the aluminum foil- and (b) the MN-surface.

The MN-surface is composed by micro-sawtooth and nano-petal structure and possesses a superhydrophobicity not only at room temperature but also at subzero temperature. Figure 3(a) shows the contact angles of the three surfaces, i.e., the MN-surface, nano-structured surface (N-surface), and blank surface (B-surface), at different temperatures ranging from −10 °C to 0 °C. The results indicate that the droplet on MN-surface can still keep in Cassie's state (superhydrophobicity, contact angle $> 150°$) at −10 °C, while this phenomenon has not appeared on the other two surfaces. On N-surface, the contact angles decrease with the decline of the temperature. On the B-surface, the state of liquid droplet changes from hydrophobicity to hydrophilicity, which is wetted by the liquid. The detachment of the liquid droplet before freezing in subzero environment is one of the most significant performances on excellent superhydrophobic and anti-icing surfaces. So, the sliding contact angle (SCA) on the surfaces were tested in Fig. 3(b). The three surfaces were placed on the cooling stage and declined the temperature from 0 °C to −10 °C (the environmental temperature was about 20 °C and the relative humidity was about 90%). From the experimental data, we assume that the temperature induces little effect to SCA on MN-surface. On MN-surface, 5 μL of the droplet can easily roll off the surface at −10 °C (SCA $< 10°$). On N-surface, the SCA of liquid droplet increases with the decline of temperature, which induces the difficulty to move the droplet off. The surface was wetted by the condensed droplets and the contact angle hysteresis increased. On the B-surface, the droplet pinned on the N-surface at subzero temperature and could not roll off at −4 °C. The droplet totally wets the surface and increases the hysteresis between solid and liquid interface. The compared experiments indicate that the MN-surface holds the best performances in low temperature. The adhesion force of the three surfaces was tested by micro-electronic balance system (Dataphysics DCAT21, Germany), which indicates that the MN-surface shows the lowest surface energy and the droplet can easily detach from the surface.

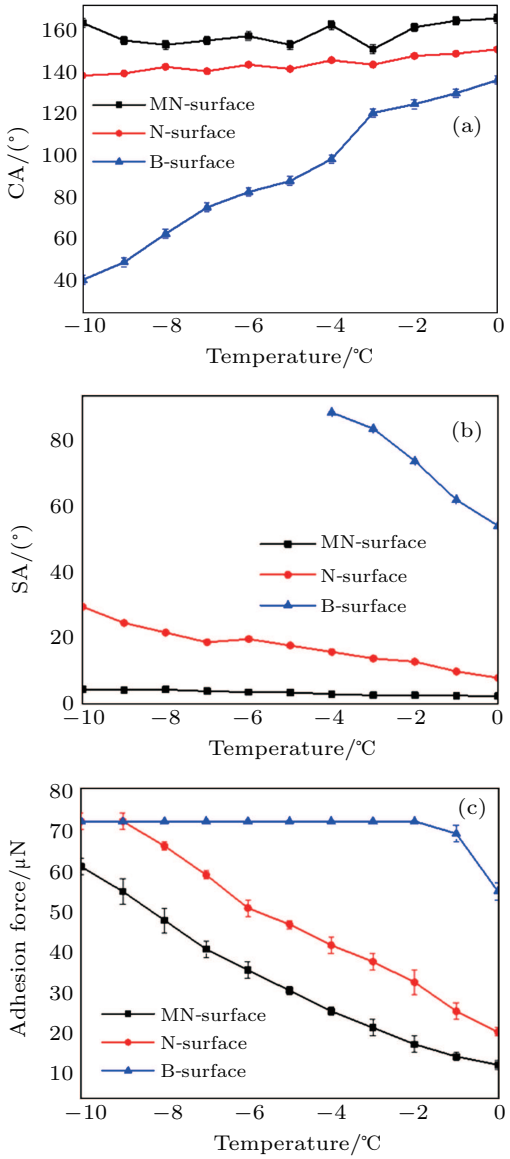


Fig. 3. (color online) The wettability test on three surfaces, i.e., MN-surface, nano-structured surface (N-surface), and blank surface (B-surface), at different temperatures ranging from −10 °C to 0 °C. (a) The contact angle, (b) the sliding contact angle analysis (SCA), and c) the adhesion force of the droplet (with size of 5 μL).

The MN-surface shows a large contact angle and a small SCA at low temperature environment, which has potential application in the ice-phobic field. The icing delay test was performed, as shown in Fig. 4. The temperature of the cooling stage was −10 °C and the relative humidity was 90%. The

droplet with a volume of 5 μL was placed on the three surfaces, i.e., MN-, N-, and B-surfaces. After about 5 min, the droplets on the B-surface froze and changed the shape from a hemisphere to a peach shape. On the N- and MN-surfaces, the droplets froze at about 20 min and 125 min, respectively. Generally, on MN-surface, the droplet still kept in Cassie's state in the freezing process and was easily blown away by the wind with speed of 0.5 m/s after melting. On the N-surface, the melted droplet could be driven off by wind with speed larger 3 m/s. On B-surface, the droplet pins to the surface and could not be removed by wind with speed larger than 10 m/s. The results indicate that the MN-surface can delay the freeze time at subzero environment.

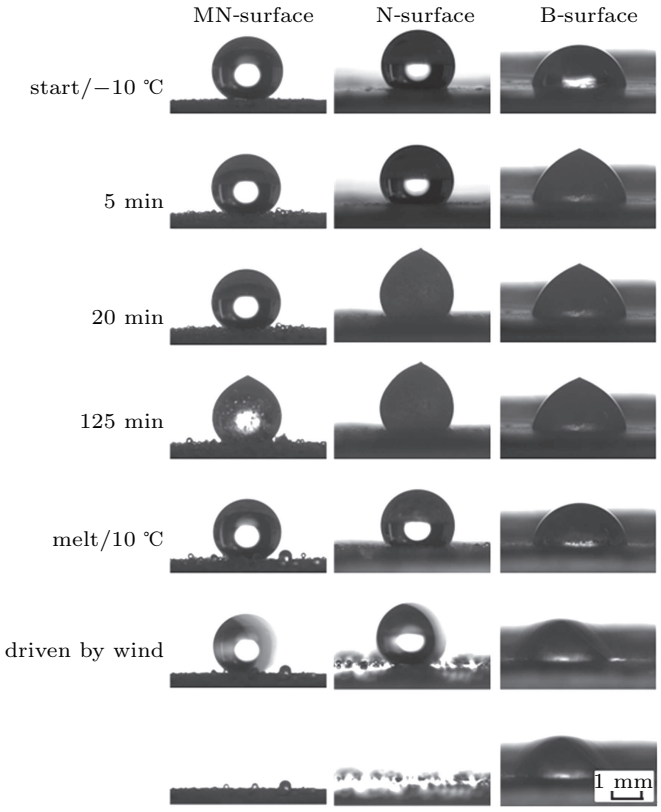


Fig. 4. The freezing process on three surfaces. The temperature of the base is 10 °C and the relative humidity is about 90%. The droplets on three surfaces, i.e., MN-, N-, and B-surfaces freeze at 125 min, 20 min, and 5 min, respectively.

To analyze the state of droplets on the different surfaces, the sketch diagram is shown in Fig. 5. At subzero and high humidity environment, the condensed droplets from the air could quickly elbow the pocketed air existing in the roughness topography and wet the surface. The stage of the droplet on the surface is changed. On the MN-surface, due to the larger roughness topography, the condensed droplets did not fill the gap between the solid and liquid interface. It is difficult to change the droplet state. The droplet with volume of 5 μL suspends on the apex region of the micro-sawtooth. With the help of the pocketed air between the base and liquid droplet, the tested droplet did not freeze at a short time. With the energy loss in low temperature, the droplet on the MN-surface solidified at 125 min. Meanwhile, the droplet kept in Cassie's state throughout the process. On the N-surface, with the decline of temperature, the condensed droplet penetrated into the gap of nano-petal structure and wet the surface, which results in wetting performance and induces the collapse of the droplet on the surface. Due to the high humidity and low temperature, the condensed droplets elbowed the air pocketing in the nano-petal and occupied the space, resulting in wetting the surface and changing the droplet stage. The stage changes from Cassie's state to Cassie–Baxter's state to Wenzel's state, which results in wetting the surface and limiting the icing delay time. On the B-surface, the droplet keeps in Wenzel's state and contacts directly with the solid surface, which induces the fast freeze in low temperature and a short time.

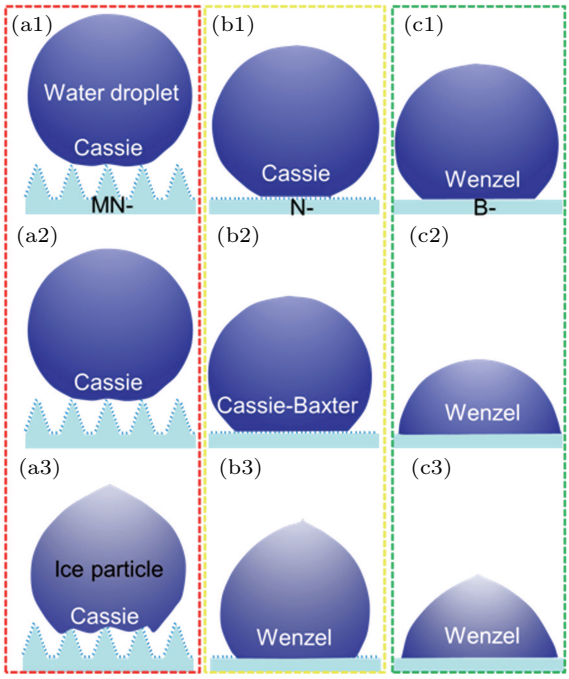


Fig. 5. (color online) The sketch diagram of the freezing process on the three surfaces. The droplet freezes on (a) MN-surface, (b) N-surface, and (c) B-surface.

4. Conclusion

In summary, an aluminum foil-based icephobic surface was prepared by the machining and crystal growth method, which consists of micro-sawtooth and ZnO nano-petal, and shows an excellent icing delay time in a low temperature environment. This method for fabricating superhydrophobic/anti-icing surface broadens the preparation of the functional material and possesses a potential application in the metal protection in the exposed environment.

References

[1] Li S M, Zhou S Z and Liu J H 2009 *Acta Phys. Chim. Sin.* **25** 2581
[2] Wang P W, Liu M J and Jiang L 2016 *Acta Phys. Sin.* **65** 186801 (in Chinese)
[3] Hao C, Liu Y, Chen X, Li J, Zhang M, Zhao Y and Wang Z 2016 *Small* **12** 1825

[4] Yu S, Guo Z and Liu W 2014 *Chem. Commun.* **51** 1775
[5] Wang L, Gao C, Hou Y, Zheng Y and Jiang L 2016 *J. Mater. Chem. A* **4** 18289
[6] Shi W, Wang L, Guo Z and Zheng Y 2015 *Adv. Mater. Interfaces* **2** 1500352
[7] Frysali M A, Papoutsakis L, Kenanakis G and Anastasiadis S H 2015 *J. Phys. Chem. C* **119** 25401
[8] Zhang W, Lin G, Li J, Xue H, Luo Y and Gao X 2015 *Adv. Mater. Interfaces* **2** 1500238
[9] Baji A, Abtahi M and Ramakrishna S 2014 *J. Nanosci. Nanotechnol.* **14** 4781
[10] Lu X, Wu Y, Cai H, Qu X, Ni L, Teng C, Zhu Y and Jiang L 2015 *RSC Adv.* **5** 54175
[11] Li H, Yu S and Han X 2015 *New J. Chem.* **39** 4860
[12] Xu Q, Li J, Tian J, Zhu J and Gao X 2014 *ACS Appl. Mater. Interfaces* **6** 8976
[13] Li J, Luo Y, Zhu J, Li H and Gao X 2015 *ACS Appl. Mater. Interfaces* **7** 26391
[14] Liu G, Li X, Wang M, Wang M, Kim J Y, Woo J Y, Wang X and Lee J K 2016 *Energ. Convers. Manag.* **126** 697
[15] Liu G C, Wang Y T, Zhang J, Wang M, Zhang C J and Wang X D 2013 *J. Chem. Technol. Biot.* **88** 818
[16] Wang Y, Liu G, Wang M, Liu G, Li J and Wang X 2013 *Int. J. Hydrogen Energ.* **38** 9000
[17] Liu G, Ding X, Zhou H, Chen M, Wang M, Zhao Z, Yin Z and Wang X 2015 *Appl. Energ.* **147** 396
[18] Tian J, Zhang Y, Zhu J, Yang Z and Gao X 2014 *ChemPhysChem* **15** 858
[19] Tian J, Zhu J, Guo H Y, Li J, Feng X Q and Gao X 2014 *J. Phys. Chem. Lett.* **5** 2084
[20] Li X, Liu G, Shi M, Zou D, Wang C and Zheng J 2016 *Sep. Purif. Technol.* **165** 154
[21] Zhao Z, Liu G, Li B, Guo L, Fei C, Wang Y, Lv L, Liu X, Tian J and Cao G 2015 *J. Mater. Chem. A* **3** 11320
[22] Li X, Liu G, Shi M, Li J, Li J, Guo C, Lee J K and Zheng J 2016 *Electrochim. Acta* **218** 318
[23] Jiang T, Guo Z and Liu W 2015 *J. Mater. Chem. A* **3** 1811
[24] Wang L, Yuan B, Lu J, Tan S, Liu F, Yu L, He Z and Liu J 2016 *Adv. Mater.* **28** 4065
[25] Yang C Y, Tsai Y L, Yang C Y, Sung C K, Yu P and Kuo H C 2014 *Appl. Phys. Express* **7** 087001
[26] Wang L, Zhang M, Gao C and Zheng Y 2016 *Adv. Mater. Interfaces* **3** 1600145
[27] Zhao R and Liang Z C 2016 *Chin. Phys. B* **25** 066801
[28] Cao S Q, Wei G H and Chen J Z Y 2015 *Chin. Phys. B* **24** 098702
[29] Li G, He D, Lin Y, Chen Z, Liu Y and Peng X 2016 *Polym. Adv. Technol.* **27** 1438
[30] Huovinen E, Takkunen L, Suvanto M and Pakkanen T A 2014 *J. Micromech. Microeng.* **24** 055017
[31] Pereira P M M, Moita A S, Monteiro G A and Prazeres D M F 2014 *J. Bionic Eng.* **11** 346
[32] Ding X, Zhou H, Liu G, Yin Z, Jiang Y and Wang X 2015 *J. Alloys Compd.* **632** 147
[33] Zhou H, Ding X, Liu G, Jiang Y, Yin Z and Wang X 2015 *Electrochim. Acta* **152** 274
[34] Zhou H, Ding X, Liu G, Gao Z, Xu G and Wang X 2015 *RSC Adv.* **5** 108007
[35] Li J, Zhang W, Luo Y, Zhu J and Gao X 2015 *ACS Appl. Mater. Interfaces* **7** 18206
[36] Zhao Y, Luo Y, Li J, Yin F, Zhu J and Gao X 2015 *ACS Appl. Mater. Interfaces* **7** 11079
[37] Wang L, Wen M, Zhang M, Jiang L and Zheng Y 2014 *J. Mater. Chem. A* **2** 3312
[38] Zhang B, Lei Q, Wang Z and Zhang X 2016 *Langmuir* **32** 346
[39] Jie H, Xu Q, Wei L and Min Y 2016 *Corros. Sci.* **102** 251
[40] Cho Y S, Moon J W, Lim D C and Kim Y D 2013 *Korean J. Chem. Eng.* **30** 1142
[41] Liu G, Peng M, Song W, Wang H and Zou D 2015 *Nano Energy* **11** 341
[42] Song W, Wang H, Liu G, Peng M and Zou D 2016 *Nano Energy* **19** 1
[43] Liu G, Gao X, Wang H, Kim A Y, Zhao Z, Lee J K and Zou D 2016 *J. Mater. Chem. A* **4** 5925